Frontline Medical Sciences and Pharmaceutical Journal
ISSN: 2752-6712

Effects of paraquat dichloride on lungs of pregnant wistar rats

Ehebha Ehizokhale Santos, MSC

Department of Human Anatomy and Cell Biology, Delta State University, Abraka, Nigeria

Obohwemu Oberhiri Kennedy, PhD

Department of Health, Wellbeing & Social Care, Global Banking School, Oxford Brookes University, Birmingham, United Kingdom; and PENKUP Research Institute, Birmingham, United Kingdom

Adesida-Ehebha Elizabeth Tolulope, MSPH

Sunderland Royal Hospital, South Tyneside and Sunderland NHS Foundation Trust, Sunderland, United Kingdom

Odokuma Emmanuel Igho, PhD

Department of Human Anatomy and Cell Biology, Delta State University Abraka, Nigeria

Ebeye Oladunni Abimbola, PhD

Department of Human Anatomy and Cell Biology, Delta State University, Abraka, Nigeria

Onomuighokpo Onome Hillary, MBBS

Department of Orthopaedics & Trauma Federal Medical Centre, Asaba, Delta State, Nigeria

Corresponding Author: Ehebha Ehizokhale Santos, MSC

ARTICLE INFO

Article history:
Submission Date: 29 December 2024
Accepted Date: 20 January 2025
Published Date: 03 February 2025
VOLUME: Vol.05 Issue02
Page No. 7-18
DOI: -
https://doi.org/10.37547/medical-fmspj-05-02-02

ABSTRACT

Introduction: Paraquat dichloride is a toxic bipyridine herbicide widely used for weed control in fruit orchards and forestry. Its fumes primarily affect the lungs due to preferential accumulation in lung alveolar cells. Aim: This study investigates paraquat toxicity in pregnant Wistar rats at varying doses over a three-week gestational period. Methods: A total of seventy-two Wistar rats were used, with 48 females entering the experimental phase after mating with males. The female rats were randomly divided into four groups: Group 1 (Normal female, n=12), Group 2 (1 mg/ml/kg bw of paraquat dichloride, n=12), Group 3 (2.5 mg/ml/kg bw, n=12), and Group 4 (5 mg/ml/kg bw, n=12). Tissues were examined weekly and prepared for histological analysis using a Primo Star ZEISS light microscope. Results: At the end of the third week, lung tissue sections exhibited varying degrees of injury, including mild inflammation, taller and slender respiratory epithelium indicating stress, bronchiolar dilation, and fibrotic changes in lung stroma. Notably, the lungs of the foetuses showed no significant histological differences compared to controls. Conclusion: Maternal exposure to paraquat during pregnancy results in dose-dependent lung

inflammation and fibrosis. Recommendations for new policies to prevent perinatal maternal exposure to paraquat are warranted.

Keywords: Gestation, Histology, Inflammation, Lung, Paraquat.

INTRODUCTION

Paraquat, a widely utilized herbicide, has consistently held a significant share of the global herbicide market. It is a quaternary nitrogen-based herbicide with a brown, syrupy liquid form (Sukumar et al., 2019; Ehebha et al., 2024), classified under bipyridinium compounds, with the chemical formula 1,1'-dimethyl-4,4'-bipyridinium (NCBI, 2025). Paraquat is used for effective weed management across various agricultural and horticultural systems, including fruit orchards, plantation crops such as coffee, cocoa, coconut, oil palm, rubber, bananas, vines, olives, and tea, as well as ornamental trees, shrubs, and forestry operations. Its efficacy makes it a vital tool in maintaining crop productivity and ecosystem management in diverse cultivation practices (Stuart et al., 2023).

Paraquat is classified by the World Health Organization (WHO) as a moderately hazardous herbicide and is categorized as a Class II poison due to its acute toxicity. This emphasizes its significant potential to cause harm upon exposure, mandating strict handling and safety measures in its application (Gawarammana & Buckley, 2011; WHO, 2023). The ingestion of even a small dose of paraquat can have fatal consequences due to its ability to induce severe pulmonary damage (Gawarammana & Buckley, 2011). Among pesticides frequently used as agents of suicide, paraquat has been identified as a major contributor to fatalities in medical centers (Gunnell & Eddleston, 2003).

Gunnell and Eddleston (2003) pointed out its significant role in mortality rates, emphasizing its severe toxicity and the challenges associated with managing paraquat poisoning in clinical settings. Paraquat poisoning becomes a serious public health problem as it has a highly toxic reaction to the body after ingestion, which can cause a series of complications, including acute respiratory distress, compression syndrome, pulmonary fibrosis, renal failure, and liver toxicity (Delirrad et al., 2015).

Despite significant variability in treatment approaches, mortality rates in cases of paraquat poisoning remain alarmingly high, ranging from 50% to 90% (Delirrad et al., 2015). The absence of an effective antidote also complicates management. Unlike organophosphate poisoning, paraquat toxicity is characterized by a potential delay of several days in the onset of clinical symptoms (Ellenhorn et al., 2018), posing additional challenges for timely diagnosis and intervention (Chypa et al., 2018; Ellenhorn et al., 2018). The clinical effects of paraquat poisoning are dose-dependent and vary according to the route of exposure (Wunnapuk et al., 2014). Higher doses and direct ingestion result in more severe toxicity, while inhalation or dermal exposure may lead to less acute manifestations but still pose significant health risks (Balali-Mood et al., 2021; Gorguner & Akgun, 2010). The severity and progression of clinical symptoms are influenced by the amount of paraquat absorbed into the system (Delirrad et al., 2015), highlighting the importance of timely intervention and the route of exposure in determining patient outcomes.

The inhalation route is the most common mode of exposure in paraquat poisoning (Kumar et al., 2016), leading to primary damage to the lungs. This is due to the accumulation of paraquat in alveolar cells, where it exerts its toxic effects, resulting in severe pulmonary injury. The lung tissue is vulnerable to oxidative stress induced by paraquat (Alizadeh et al., 2022; Memarzia et al., 2024), contributing to the development of acute respiratory distress syndrome (ARDS) and other pulmonary complications (Matthay et al., 2019; Swenson & Swenson, 2021).

Paraquat causes progressive and irreversible pulmonary damage, primarily through the generation of reactive oxygen species (ROS) that induce oxidative stress in lung tissue (Alizadeh et al., 2022). This leads to the gradual development of pulmonary fibrosis, severely impairing lung function and often resulting in respiratory failure. The irreversible nature of this damage indicates the urgent need for early detection and intervention in cases of paraquat poisoning to prevent long-term morbidity (Gawarammana & Buckley, 2011).

Paraquat exhibits the highest concentrations (ranging from 0.01% to 0.02%) in the lungs, liver, and kidneys (Abdul et al., 2021), where it accumulates following systemic absorption. This

accumulation in vital organs contributes to the severity of toxic effects, particularly in the lungs, leading to pulmonary fibrosis (Wu et al., 2022), and in the liver causing hepatotoxicity (Ehebha et al., 2024) and kidneys causing nephrotoxicity (Balali-Mood et al., 2021; Chen et al., 2021).

Ingestion of large amounts of paraquat leads to widespread systemic toxicity, resulting in multiple organ failure and, if untreated, death (Lin et al., 2021). The accumulation of paraquat in key organs such as the lungs, liver, and kidneys precipitates severe damage (Asaduzzaman et al., 2021; Ehebha et al., 2024), overwhelming the body's physiological systems and often leading to irreversible organ dysfunction. The rapid progression of toxicity underscores the importance of early diagnosis and intervention in mitigating fatal outcomes (Asim et al., 2020).

Ingestion of moderate amounts of paraquat can result in severe complications, including renal failure, massive pulmonary fibrosis, cardiac arrhythmias, and oesophageal perforation (Sukumar et al., 2019), all of which significantly increase the risk of death. The accumulation of paraquat in the lungs and kidneys leads to progressive organ damage, while systemic effects such as arrhythmias and gastrointestinal injury further exacerbate the critical condition of the patient (Asaduzzaman et al., 2023). Without prompt and effective intervention, these multifactorial toxic effects often culminate in fatal outcomes (Tejo et al., 2023).

Paraquat is primarily used for deliberate self-harm or suicide in developing countries, as reported by Myung et al. (2015) and Delirrad et al. (2015). However, other studies have indicated that paraquat was responsible for more deaths than any other pesticide in 2008 in the United States, accentuating its global impact as a significant cause of pesticide-related fatalities (Gawarammana & Buckley, 2011). This affirms the need for international attention and regulatory measures to mitigate the risks associated with paraquat use (Kim et al., 2009; Lee et al., 2017). Due to its high toxicity and associated health risks, the European Union took the precautionary step of withdrawing paraquat from its market in July 2007. This regulatory action reflects the growing concerns about the herbicide's potential for misuse and its severe toxicological effects on human health, prompting the need for safer alternatives in agricultural and industrial applications (Gawarammana & Buckley, 2011; Kervegant et al., 2013).

This study aimed to histologically evaluate the lungs of Wistar rats exposed to varying doses of paraquat dichloride, assessing the extent of pulmonary damage and characterizing the morphological changes induced by different levels of paraquat exposure on lung tissue throughout the gestational period. Previous literature has demonstrated the effect of paraquat on the lungs of male Wistar rats (Jurima & Shek, 1990) and non-gravid female Wistar rats (Ali et al., 2000). However, this study highlights the effects of paraquat on the lungs of pregnant Wistar rats, examining the histological effects.

MATERIALS AND METHODS

Reagents: The reagents used in this study include paraquat dichloride, normal saline, paraffin wax, 10% formaldehyde saline, 70% ethanol, 90% alcohol, 95% alcohol, absolute alcohol, xylene, and haematoxylin and eosin stain.

Animals: Forty-eight (48) female Wistar rats were obtained and bred in the Animal Laboratory Centre, Faculty of Basic Medical Science, Delta State University, Abraka. The animals were allowed two weeks to acclimatize, with free access to normal rat feed and clean drinking water ad libitum.

Animal Grouping and Administration of Paraquat via Orogastric Tube:

- Group 1: Control (n = 12; divided equally into 3 sub-groups (n = 4) for weekly study over a 3-week period)
- Group 2: 1 mg/ml of paraquat dichloride (n = 12; divided equally into 3 sub-groups (n = 4) for weekly study over a 3-week period)
- Group 3: 2.5 mg/ml of paraquat dichloride (n = 12; divided equally into 3 sub-groups (n = 4) for weekly study over a 3-week period)
- Group 4: 5 mg/ml of paraquat dichloride (n = 12; divided equally into 3 sub-groups (n = 4) for weekly study over a 3-week period)

The presence of a sperm plug in the vagina of the female rats was considered the first day of gestation, from which the administration of paraquat dichloride commenced. Rats were euthanized weekly (n = 4/group) over a 3-week period (n = 12/group in total).

Collection of Samples: The rats were euthanized by cervical dislocation to prevent chemical influence on the expected results of the biochemical analysis. The rats were dissected, and internal organs exposed. The lungs were excised and fixed immediately in 10% formal saline.

Tissue Processing: After dissection, tissue sections

from the harvested lungs were placed in tissue cassettes and processed manually under standard histological procedures, which include stages from fixation to mounting. Slides were viewed with a binocular light microscope. The findings were interpreted to determine the histological effect of paraquat on the lungs of the pregnant Wistar rats. Photomicrographs were obtained from all the groups.

Ethical Approval: Ethical approval was obtained from the Research and Bio-Ethics Committee of the Faculty of Basic Medical Sciences, Delta State University, Abraka, Delta State, with reference number REC/FMS/DELSU/22/166. All animals used in this study were handled according to standard protocols for the use of laboratory animals as outlined by the Committee.

Micrograph Reporting: The results obtained were reported by the principal investigator and confirmed by a pathologist. The results were presented in well-labelled plates for the histological slides.

RESULTS

Photomicrographs

Samples were taken from each group at the end of weeks one, two, and three, and the tissues were prepared for examination under a Primo Star ZEISS light microscope. For the adult, pregnant Wistar rats, the photomicrographs acquired were exhibited and reported weekly for the lungs.

Week One

Histological analysis of pregnant Wistar rat lung tissues. Note: The rat lung tissues were stained with haematoxylin and eosin.

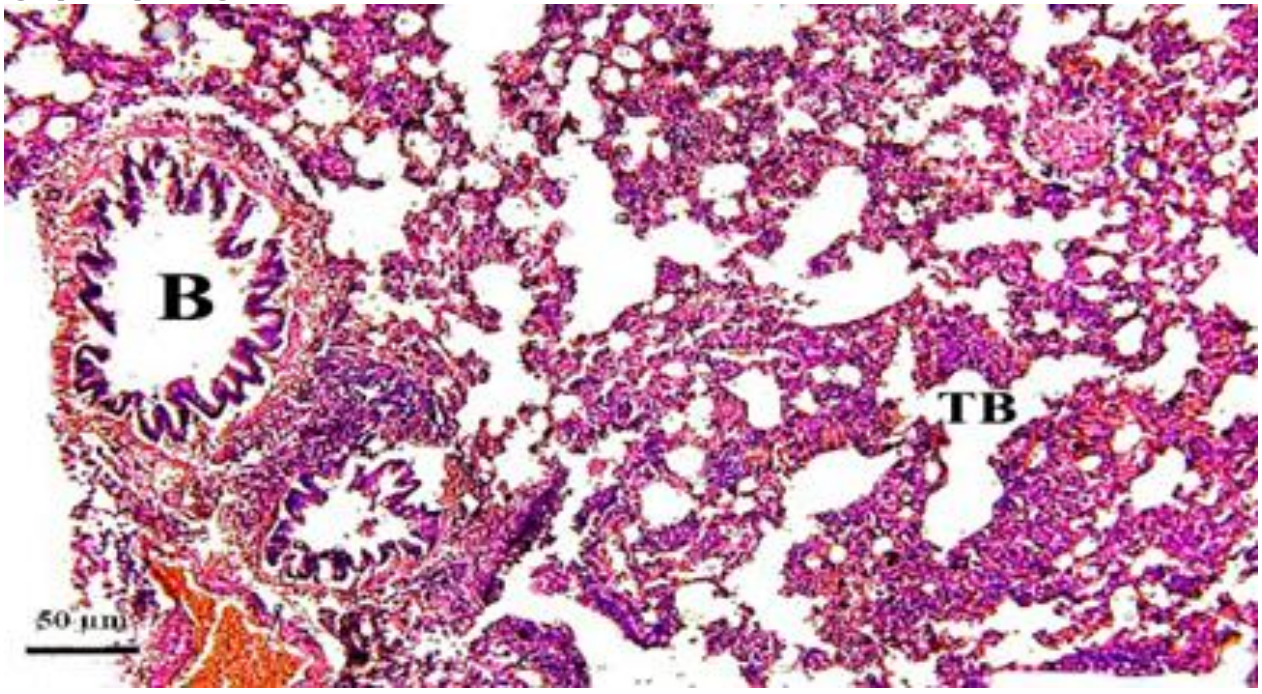

Figure 1a: Group One (Control) H&E stain x100

The section of the lungs displayed bronchioles interspersed among alveoli, comprising an epithelial surface, supporting tissue, and blood vessels. The bronchiole includes both a terminal and a respiratory portion, which is clearly seen. Also displayed is a bronchus (B). Noticeably, the cells lining the alveoli are flat and in a single layer—squamous. The smooth muscular wall of the bronchiole is lined by simple columnar ciliated cells in the clear lumen, supported by a lamina propria. Some neutrophils and a blood vessel can also be spotted. Features display normal lung tissue.

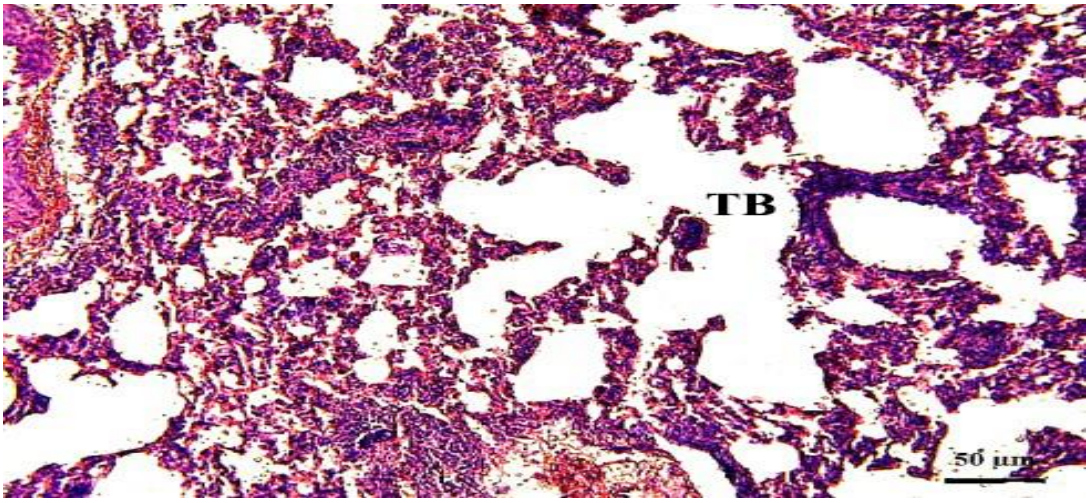

Figure 1b: Group Two (Test 1 mg/ml/kg.bw PQ) H&E stain x100

The lung tissues indicate that the terminal bronchioles (TB) leading to the alveoli sac are dispersed on the micrograph. Cells lining the alveoli are flat and in a single layer—squamous. The smooth muscular wall of the bronchiole is lined by simple columnar ciliated cells facing the clear lumen. Some neutrophils and macrophages can also be spotted.

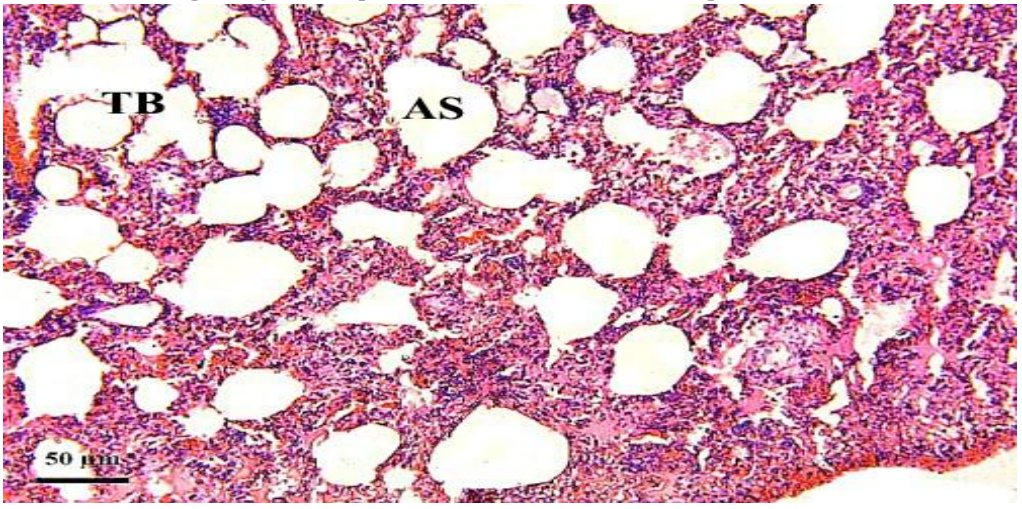

Figure 1c: Group Three (Test 2.5 mg/ml/kg.bw PQ) H&E stain x100

The lungs show the terminal bronchioles (TB) leading to the alveoli sac, which are more dispersed on the micrograph, while some alveoli show collapsed features compared with the control and Group 2. Cells lining the alveoli are flat and in a single layer—squamous. Some exhibit irregularities due to visible fracture. The bronchiole is unchanged.

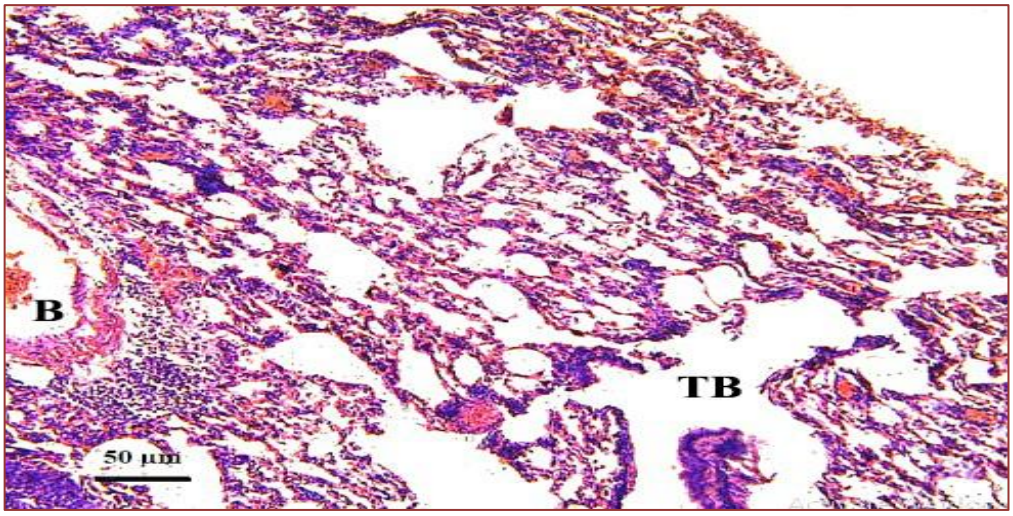

Figure 1d: Group Four (Test 5 mg/ml/kg.bw PQ) H&E stain x100

The lung displayed the terminal bronchioles (TB) leading to the alveoli sac, showing thicker walls and high basophilic staining on this micrograph—a response to injury. Cells lining the alveoli are flat and in a single layer—squamous, showing discontinuation and collapse. The smooth muscular wall of the bronchiole is thinner than in the control. Some neutrophils can also be spotted.
Key: PQ – Paraquat, TB - terminal bronchioles, BV - blood vessels, B - bronchus, AS - alveoli sac
Week Two

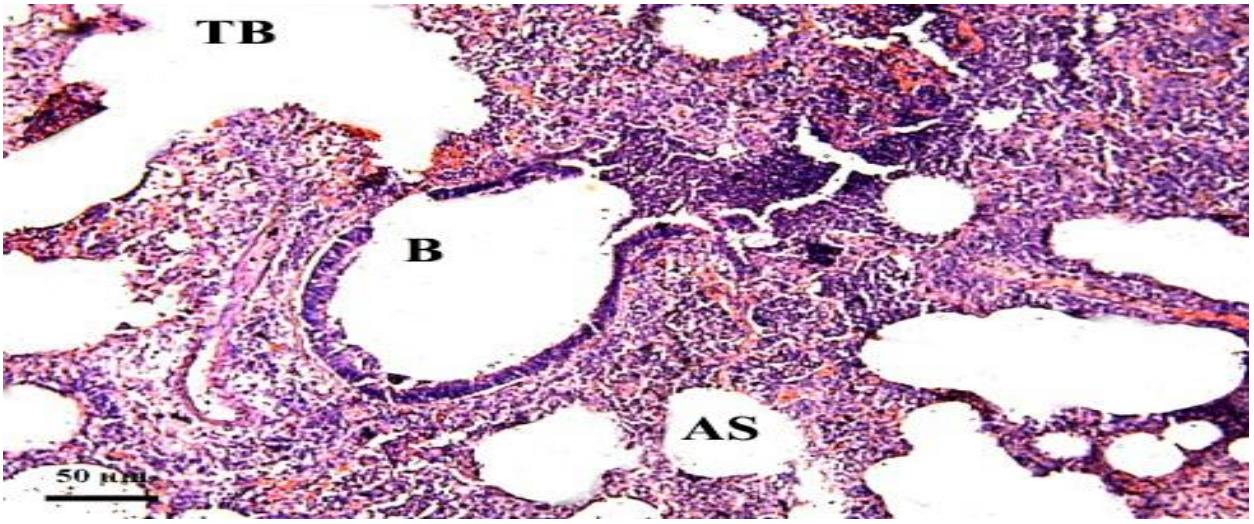

Figure 2a: Group One (Control) H&E stain x100

The bronchiole (B) and terminal bronchioles (TB) are seen. The alveoli sacs are dispersed on the micrograph. Cells lining the alveoli are flat and in a single layer of squamous epithelium. The smooth muscular wall of the bronchiole is seen, lined by simple columnar ciliated cells in the clear lumen. Some neutrophils and a blood vessel can also be spotted.

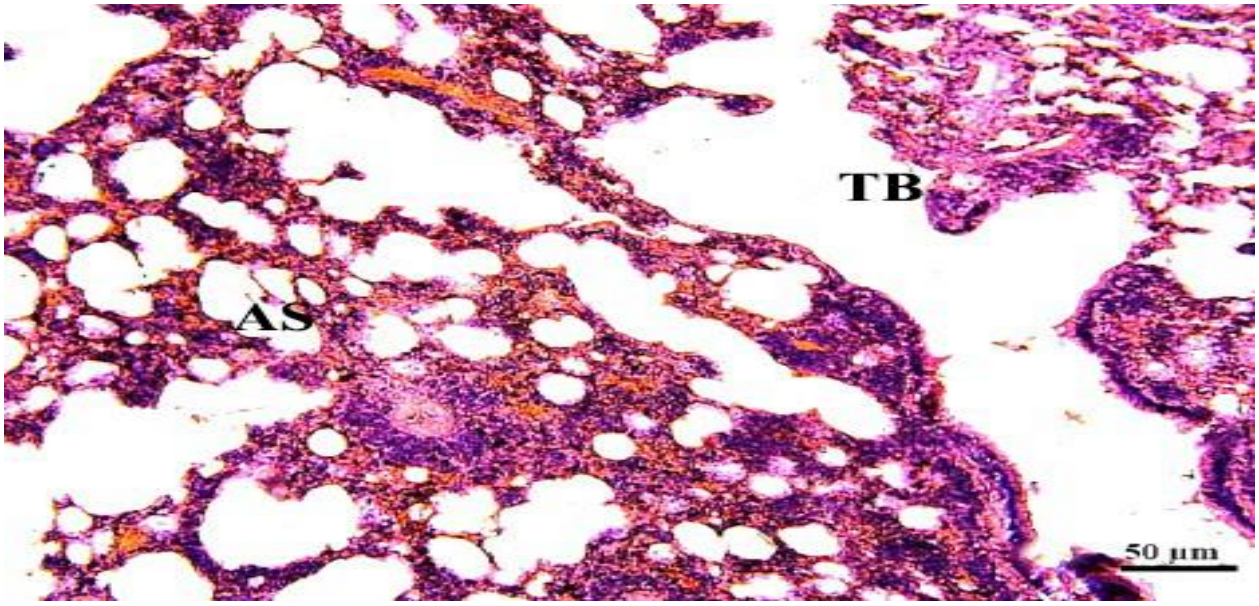

Figure 2b: Group Two (Test 1 mg/ml/kg.bw PQ) H&E stain x100

The terminal bronchioles (TB) leading to the alveoli sacs are dispersed on the micrograph. They are lined by normal respiratory epithelium. Squamous cells lining the alveoli are in a single layer. The increased number of alveoli shows a compensatory mechanism. Some neutrophils and macrophages can also be spotted.

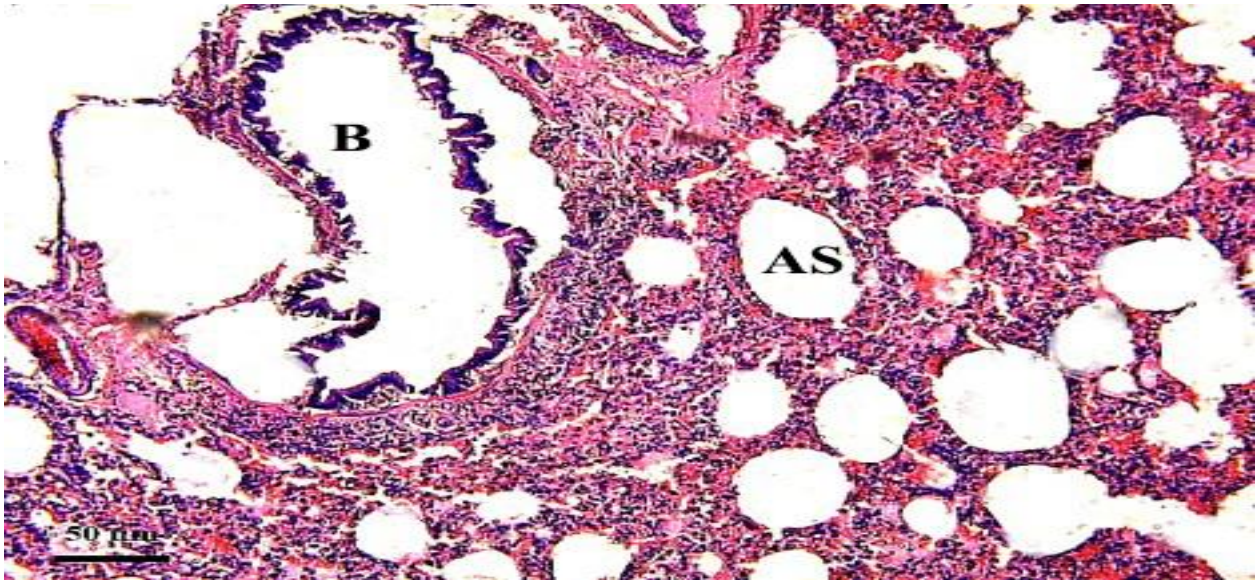

Figure 2c: Group Three (Test 2.5 mg/ml/kg.bw PQ) H&E stain x100

The alveoli sacs are more numerous on this micrograph. Some alveoli show normal features, but a small amount of fibrosis is seen compared to the control and Group 2. Cells lining the alveoli are flat and in a single layer—squamous. The bronchiole appears to be collapsing. A congested blood vessel is seen.

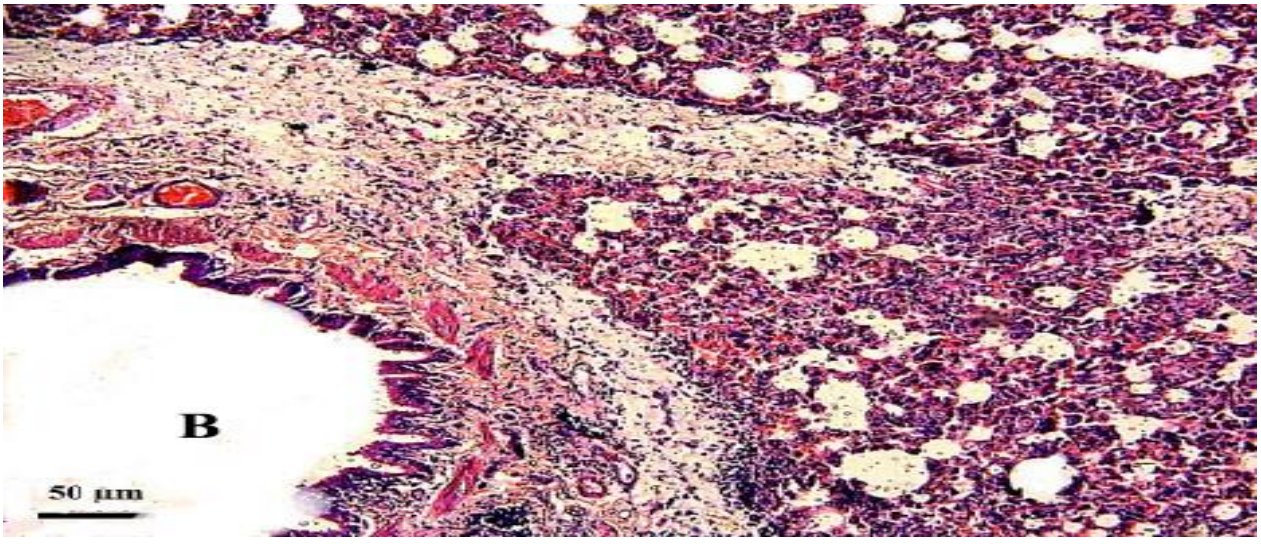

Figure 2d: Group Four (Test 5 mg/ml/kg.bw PQ) H&E stain x100

The terminal bronchioles (TB) leading to the alveoli sac show thicker walls and high basophilic staining on this micrograph (response to injury). Cells lining the alveoli are flat and in a single layer. There are signs of collapse. The smooth muscular wall of the bronchiole is in small groups with a discontinuous appearance. There are signs of fibrosis of the lung tissue parenchyma, which were not seen in the control. Some neutrophils can also be spotted.

Histologic analysis of pregnant Wistar rat lungs in the second week of the experiment. Note: The rat lung tissues were stained with hematoxylin and eosin.

Key: PQ – Paraquat, TB - terminal bronchioles, BV - blood vessels, B - bronchus, AS - alveoli sac

Week Three

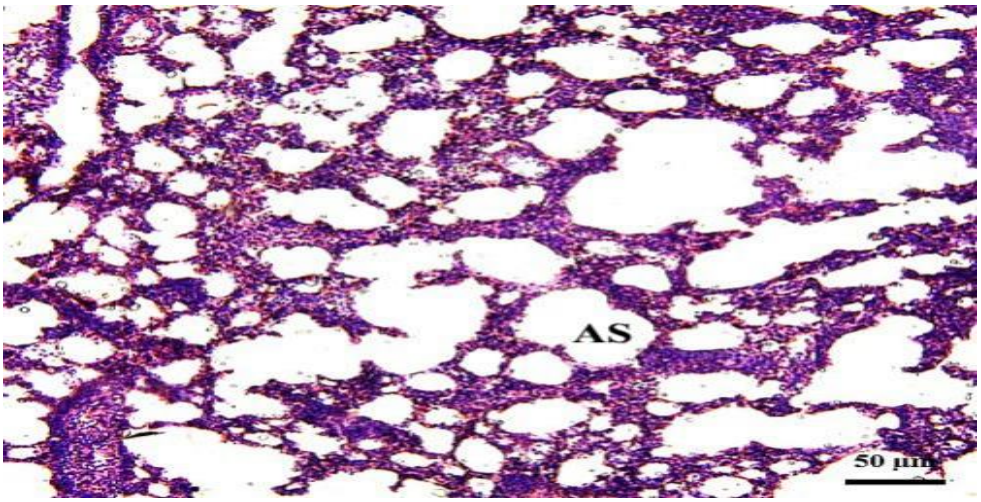

Figure 3a: Group One (Control) H&E stain x100
Sections of the lungs display alveoli sacs of variable sizes. Also displayed are terminal and respiratory bronchioles. Flattened cells lining the alveoli of the lung are seen. These cells appear to be round to oval with vesicular nuclei positioned in the cytoplasm of the cell.

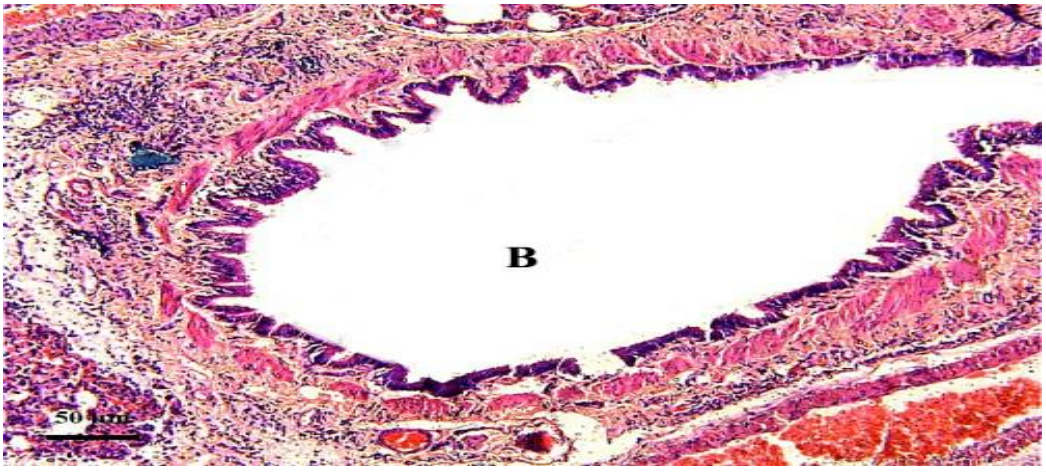

Figure 3b: Group Two (Test 1 mg/ml PQ) H&E
stain x100 Sections of the lung show an obvious bronchus, lined by respiratory epithelium, interspersed with columnar cells. These cells are slender and tall, positioned in their cytoplasm. Also seen is a muscular layer supporting the epithelium, composed of multiple muscle fiber layers. There is also the presence of a blood vessel.

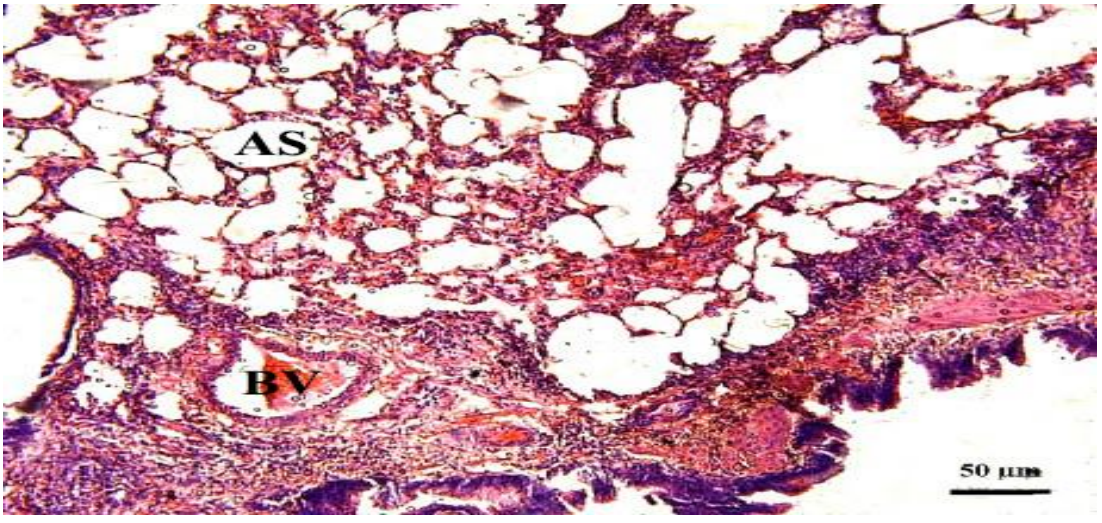

Figure 3c: Group Three (Test 2.5 mg/ml) H&E stain x100 Lung tissue sections display alveoli sacs of

variable sizes. Also seen are terminal and respiratory bronchioles interspersed among alveoli sacs. Flattened cells lining the alveoli of the lung are seen. These cells appear to be round to oval with vesicular nuclei positioned in the cytoplasm of the cell. Also seen are blood vessels filled with blood, clearly showing their tunics: intima, media, and adventitia.

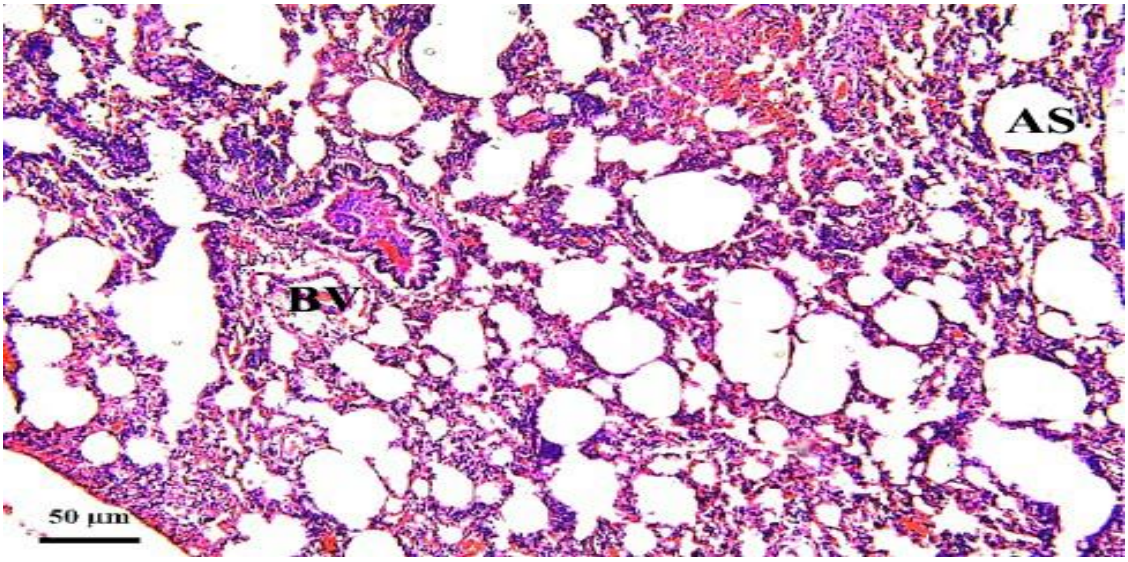

Figure 3d: Group Four (Test 5 mg/ml PQ) H&E stain x100 Lung sections reveal variably sized alveoli sacs, with bronchioles showing their terminal and respiratory portions. Also captured is the bronchus, focused and slightly pushed to the left side of the section. Cellular features seen in the alveoli are displayed in the alveoli sac, with round to oval vesicular nuclei positioned in basophilic cytoplasm.

Key: PQ – Paraquat, TB - terminal bronchioles, BV - blood vessels, B- bronchus, AS- alveoli sac

DISCUSSION

This research aimed to investigate the histological effects of paraquat dichloride (PQ) on the lungs of pregnant Wistar rats. The study was conducted in the Histology Laboratory of the Department of Human Anatomy and Cell Biology, Faculty of Basic Medical Sciences. The experimental design involved administering varying doses of paraquat (1 mg/ml, 2.5 mg/ml, and 5 mg/ml) over a 21-day gestational period to pregnant Wistar rats. The rats were divided into four groups: Group 1 served as the control (no paraquat administered), while Groups 2, 3, and 4 received paraquat at different doses. After the exposure period, lung tissue samples from all groups were collected, processed, and examined microscopically. The histological findings were compared with those of the control group to assess the impact of paraquat on lung tissue structure.

The histological results, illustrated in Figures for weeks 1, 2, and 3, revealed a dose-dependent progression of lung tissue damage. In Week 1, mild fibrosis, alveolar sac collapse, and bronchiolar dilation were observed, with the severity of these changes correlating directly with the dose of paraquat administered, similar to the patterns reported in previous acute toxicity studies by Corrin & Nicholson (2011). In Week 2, more tissue damage was observed, with the collapse of two alveolar sacs, indicating moderate lung injury. By Week 3, significant fibrosis of the lung tissues and thickening of the alveolar walls were evident, further reducing the space available for respiration.

These findings are consistent with those of previous studies that reported similar pathological changes in the lungs of Wistar rats, monkeys, and dogs following exposure to paraquat (Dinis et al., 2007; Shao et al., 2022). However, some studies have reported findings that do not fully align with the observations made in this study. It is important to note that the lung tissue damage observed here is dose-dependent, with the severity of the injury correlating with the administered dose of paraquat. This result also supports the findings of Gawarammana & Buckley (2011), who studied the management of paraquat ingestion and noted similar effects on lung tissues. Sukumar et al. (2019) in their research also revealed similar pulmonary damage, corroborating the toxic effects of paraquat. This could be attributed to the fact that paraquat accumulates in the lungs, as demonstrated through tissue distribution studies

(Yang et al., 2023), as they are the first organ to be exposed to the chemical before it is distributed to other parts of the body. The lungs have a high affinity for paraquat, as established through radioisotope tracking studies (Dinis-Oliveira et al., 2008), and as the primary organ for respiration, they are particularly susceptible to inhalation injuries caused by toxic chemicals like paraquat.

While Wistar rats have a gestation period that differs significantly from that of humans, their pregnancy can be divided into three trimesters, each lasting approximately one week (Patten et al., 2014). The physiological changes during rat pregnancy have been well documented in developmental biology literature (De et al., 2002). In this study, the rats were grouped into three experimental groups, with each group receiving paraquat doses of 1 mg/ml, 2.5 mg/ml, and 5 mg/ml during each respective trimester. The lower dose (1 mg/ml) administered to the rats during the first trimester did not produce significant lung damage. However, further exposure to 2.5 mg/ml paraquat resulted in more obvious lung injury, which was further exacerbated when the 5 mg/ml dose was administered during the second trimester.

At the higher dose of 5 mg/ml, the histological findings demonstrated more severe lung tissue damage, with marked fibrosis, bronchiolar dilation, and thickening of alveolar walls, consistent with the dose relationship established in previous studies (Corrin & Nicholson, 2011). This study found that the second trimester of pregnancy was particularly sensitive to paraquat exposure, which could be attributed to both the increase in the dose of paraquat and the unique physiological conditions of this developmental stage. The respiratory epithelium exhibited signs of stress, with cells becoming taller and slender, indicative of cellular hyperplasia and a reactive response to the toxic injury, as characterized in previous studies (Kia & Bajaj, 2023). Bronchiolar dilation and a fibrotic transformation of the lung stroma were observed. These structural changes are consistent with the early stages of pulmonary fibrosis, a hallmark of paraquat toxicity.

The findings of this study contribute to a deeper understanding that paraquat-induced lung injury is primarily mediated through the generation of reactive oxidative species (ROS), as stated by studies involving molecular pathways (Kellner et al., 2017), which cause oxidative stress and tissue damage. The ROS generation damages cellular components, such as lipids, proteins, and DNA, leading to inflammation, cell death, and subsequent fibrosis, as indicated through biochemical studies (Juan et al., 2021). In the lungs, this oxidative stress activates signaling pathways that promote the excessive deposition of collagen, leading to the thickening of alveolar walls and the characteristic fibrotic changes observed in this study, consistent with the mechanisms of fibrotic progression (Bezerra et al., 2023).

CONCLUSION

This study observed significant histological damage caused by varying doses of paraquat dichloride on the lungs of pregnant Wistar rats. The dose-dependent lung injury, ranging from mild fibrosis to severe pulmonary fibrosis and alveolar collapse, emphasizes the toxic effects of paraquat, especially during critical stages of gestation. Exposure to paraquat resulted in progressive lung tissue damage, including bronchiolar dilation, alveolar collapse, and fibrosis, with the most severe changes occurring at the highest dose (5 mg/ml) during the second trimester. These findings are consistent with previous studies on paraquat-induced pulmonary injury in different species, further stressing the importance of early intervention to reduce long-term effects.

The study also indicates that the timing of exposure during pregnancy plays a significant role in the extent of pulmonary damage, particularly during organogenesis. Considering the irreversible nature of paraquat-induced lung damage and its potential risks to human health, particularly during pregnancy, this study underscores the need for caution in its use. Further research is essential to identify potential therapeutic interventions and to promote safer agricultural practices to minimize the harmful effects of paraquat exposure.

Lawmakers are urged to create favourable policies to protect farmers who are pregnant or intend to get pregnant and are using paraquat as a weed killer. These policies should aim to protect them or reduce the amount of herbicide they are exposed to.

CONFLICTS OF INTEREST

The authors report no conflicts of interest.

FUNDING

This research did not receive any grant from funding agencies in the public, commercial, or not-

for-profit sectors.

ACKNOWLEDGEMENT

The authors would like to acknowledge the management and technical staff of PENKUP Research Institute, Birmingham, UK, for their excellent assistance and for providing medical writing and editorial support in accordance with Good Publication Practice (GPP3) guidelines.

REFERENCES

1. Abdul, K. S. M., De Silva, P. M. C. S., Ekanayake, E. M. D. V., Thakshila, W. A. K. G., Gunarathna, S. D., Gunasekara, T. D. K. S. C., Jayasinghe, S. S., Asanthi, H. B., Chandana, E. P. S., Chaminda, G. G. T., Siribaddana, S. H., & Jayasundara, N. (2021). Occupational Paraquat and Glyphosate Exposure May Decline Renal Functions among Rural Farming Communities in Sri Lanka. International journal of environmental research and public health, 18(6), 3278.
2. Ali, S., Diwakar, G., & Pawa, S. (2000). Paraquat induces different pulmonary biochemical responses in Wistar rats and Swiss mice. Chemico-biological interactions, 125(2), 79–91.
3. Alizadeh, S., Anani-Sarab, G., Amiri, H., & Hashemi, M. (2022). Paraquat induced oxidative stress, DNA damage, and cytotoxicity in lymphocytes. Heliyon, 8(7), e09895.
4. Asaduzzaman, M., Roy, S., Das Pew, N., Roy, A. D., Kibria, S., Roy, R. K., Alam, M. M. J., & Chakraborty, S. R. (2023). Paraquat induced acute kidney and lung injury with a dramatic response to methylprednisolone: A case report. Toxicology reports, 11, 350–354.
5. Asaduzzaman, M., Chando, M. R., Ahmed, N., Rezwanul Islam, K. M., Alam, M. M. J., & Roy, S. (2021). Paraquat-induced acute kidney and liver injury: Case report of a survivor from Bangladesh. Clinical case reports, 9(11), e05020.
6. Balali-Mood, M., Naseri, K., Tahergorabi, Z., Khazdair, M. R., & Sadeghi, M. (2021). Toxic Mechanisms of Five Heavy Metals: Mercury, Lead, Chromium, Cadmium, and Arsenic. Frontiers in pharmacology, 12, 643972.
7. Bezerra, F. S., Lanzetti, M., Nesi, R. T., Nagato, A. C., Silva, C. P. E., Kennedy-Feitosa, E., Melo, A. C., Cattani-Cavalieri, I., Porto, L. C., & Valenca, S. S. (2023). Oxidative Stress and Inflammation in Acute and Chronic Lung Injuries. Antioxidants (Basel, Switzerland), 12(3), 548. https://doi.org/10.3390/antiox12030548
8. Chyka P, Holstege C, Henretig F Year: (2018) Diagnosis and treatment of acute poisoning: a review" Journal of Medical Toxicology Vol: 14 (4) 310-331
9. Clarke, G. M., Conti, S., Wolters, A. T., & Steventon, A. (2019). Evaluating the impact of healthcare interventions using routine data. BMJ (Clinical research ed.), 365, l2239.
10. Corrin, B., & Nicholson, A. G. (2011). Acute alveolar injury and repair. Pathology of the Lungs, 135–153.
11. de Rijk, E. P., van Esch, E., & Flik, G. (2002). Pregnancy dating in the rat: placental morphology and maternal blood parameters. Toxicologic pathology, 30(2), 271–282.
12. Delirrad, M., Majidi, M., & Boushehri, B. (2015). Clinical features and prognosis of paraquat poisoning: a review of 41 cases. International journal of clinical and experimental medicine, 8(5), 8122–8128.
13. Dinis-Oliveira, R. J., Duarte, J. A., Sánchez-Navarro, A., Remião, F., Bastos, M. L., & Carvalho, F. (2008). Paraquat poisonings: mechanisms of lung toxicity, clinical features, and treatment. Critical reviews in toxicology, 38(1), 13–71.
14. Eddleston, M., Buckley, N. A., Eyer, P., & Dawson, A. H. (2008). Management of acute organophosphorus pesticide poisoning. Lancet (London, England), 371(9612), 597–607.
15. Ehebha, E. S., Ahama. E. E., Odokuma. I. E. (2024). Histopathological effecys of paraquat dichloride on the liver of pregnant wistar rats at various trimesters. Egypt j. forensic Sci. Appli. Toxicol, 24(3), 121-127.
16. Gorguner, M., & Akgun, M. (2010). Acute inhalation injury. The Eurasian journal of medicine, 42(1), 28–35.
17. Gunnell, D., & Eddleston, M. (2003). Suicide by intentional ingestion of pesticides: a continuing tragedy in developing countries. International journal of epidemiology, 32(6), 902–909.
18. Juan, C. A., Pérez de la Lastra, J. M., Plou, F. J., & Pérez-Lebeña, E. (2021). The Chemistry of Reactive Oxygen Species (ROS) Revisited: Outlining Their Role in Biological Macromolecules (DNA, Lipids and Proteins) and Induced Pathologies. International journal of molecular sciences, 22(9), 4642.
19. Jurima-Romet, M., & Shek, P. N. (1990). Biochemical changes in rat lung during acute paraquat intoxication. Biomedical and environmental sciences: BES, 3(3), 343–352.
20. Kervégant, M., Merigot, L., Glaizal, M., Schmitt,

C., Tichadou, L., & de Haro, L. (2013). Paraquat poisonings in France during the European ban: experience of the Poison Control Center in Marseille. Journal of medical toxicology: official journal of the American College of Medical Toxicology, 9(2), 144–147.

21. Kia'i N, Bajaj T. Histology, Respiratory Epithelium. [Updated 2023 May 1]. In: StatPearls [Internet]. Treasure Island (FL): StatPearls Publishing; 2025 Jan.

22. Kellner, M., Noonepalle, S., Lu, Q., Srivastava, A., Zemskov, E., & Black, S. M. (2017). ROS Signaling in the Pathogenesis of Acute Lung Injury (ALI) and Acute Respiratory Distress Syndrome (ARDS). Advances in experimental medicine and biology, 967, 105–137.

23. Kim, S.J., Gil, H.W., Yang, J.O., Lee, E.Y. and Hong, S.Y. (2009). The clinical features of acute kidney injury in patients with acute paraquat intoxication. Nephrol Dial Transplant 24:1226-32

24. Kumar, H., Singh, V. B., Meena, B. L., Gaur, S., & Singla, R. (2016). Paraquat Poisoning: A Case Report. Journal of clinical and diagnostic research: JCDR, 10(2), OD10–OD11.

25. Lee, E., Seo, M. S., Kim, S., Lee, D., Lee, J. Y., & Park, S. (2017). Clinical characteristics and outcomes of acute kidney injury in patients with paraquat poisoning. Journal of Korean Medical Science, 32(9), 1512-1519. Link to Google Scholar.

26. Lin, C. C., Hsu, K. H., Shih, C. P., & Chang, G. J. (2021). Hemodynamic and electromechanical effects of paraquat in rat heart. PloS one, 16(4), e0234591.

27. Matthay, M. A., Zemans, R. L., Zimmerman, G. A., Arabi, Y. M., Beitler, J. R., Mercat, A., Herridge, M., Randolph, A. G., & Calfee, C. S. (2019). Acute respiratory distress syndrome. Nature reviews. Disease primers, 5(1), 18

28. Myung, W., Lee, G. H., Won, H. H., Fava, M., Mischoulon, D., Nyer, M., Kim, D. K., Heo, J. Y., & Jeon, H. J. (2015). Paraquat prohibition and change in the suicide rate and methods in South Korea. PloS one, 10(6), e0128980.

29. National Center for Biotechnology Information (2025). PubChem Compound Summary for CID 18179176, 1,1-Dimethyl-4,4-bipyridinium dichloride. Retrieved January 8, 2025

30. Patten, A. R., Fontaine, C. J., & Christie, B. R. (2014). A comparison of the different animal models of fetal alcohol spectrum disorders and their use in studying complex behaviors. Frontiers in pediatrics, 2, 93.

31. Shao, M., Yang, S., Zheng, A., Wu, Z., Chen, M., Yao, R., Shi, Y., & Chen, G. (2022). Pathophysiological Changes in Rhesus Monkeys with Paraquat-Induced Pulmonary Fibrosis. Lung, 200(5), 549–560.

32. Stuart, A. M., Merfield, C. N., Horgan, F. G., Willis, S., Watts, M. A., Ramírez-Muñoz, F., U, J. S., Utyasheva, L., Eddleston, M., Davis, M. L., Neumeister, L., Sanou, M. R., & Williamson, S. (2023). Agriculture without paraquat is feasible without loss of productivity-lessons learned from phasing out a highly hazardous herbicide. Environmental science and pollution research international, 30(7), 16984–17008.

33. Sukumar, C. A., Shanbhag, V., & Shastry, A. B. (2019). Paraquat: The Poison Potion. Indian journal of critical care medicine: peer-reviewed, official publication of Indian Society of Critical Care Medicine, 23(Suppl 4), S263–S266. Swenson, K. E., & Swenson, E. R. (2021). Pathophysiology of Acute Respiratory Distress Syndrome and COVID-19 Lung Injury. Critical care clinics, 37(4), 749–776.

34. Tejo, A. M., Hamasaki, D. T., Menezes, L. M., & Ho, Y. L. (2023). Severe dengue in the intensive care unit. Journal of intensive medicine, 4(1), 16–33.

35. World Health Organization, WHO (2023). World Malaria Report 2022. WHO, Geneva

36. Wu, Y., Li, N., Li, S., & Song, S. (2022). Lung transplantation in a woman with paraquat poisoning that led to pulmonary Fibrosis-Widely reported by the media: A case report. Medicine, 101(49), e32263.

37. Wunnapuk, K., Mohammed, F., Gawarammana, I., Liu, X., Verbeeck, R. K., Buckley, N. A., Roberts, M. S., & Musuamba, F. T. (2014). Prediction of paraquat exposure and toxicity in clinically ill poisoned patients: a model-based approach. British journal of clinical pharmacology, 78(4), 855–866.

38. Yang, X., Xiao, P., & Shi, X. (2023). Molecular mechanism of paraquat-induced ferroptosis leading to pulmonary fibrosis mediated by Keap1/Nrf2 signalling pathway. Molecular biology reports, 50(11), 9249–92.